

Synthesis, anti-lung cancer activity and molecular docking study of 3-methylene-2-oxoindoline-5-carboxamide derivatives

Juntao Ai¹ · Meng Lv¹ · Xiaohui Li² · Zhuo Chen¹ · Gaoyun Hu¹ · Qianbin Li¹

Received: 8 May 2017 / Accepted: 24 August 2017
© Springer Science+Business Media, LLC 2017

Abstract A series of 3-methylene-2-oxoindoline-5-carboxamide derivatives were synthesized in appreciable yield by using 4-aminobenzoic acid as a starting material. The preliminary biological test results showed that most compounds displayed potent inhibitory activity against proliferation of human lung adenocarcinoma epithelial cell line (A549) in MTT assay. Compound **6l** displayed the highest potency ($IC_{50} = 3.0 \mu\text{M}$). The western blot analysis demonstrated a correlation between anti-proliferative activity of active compounds and blockade of the phosphorylation of extracellular signal-regulated kinases (ERK1/2). The docking study also provides new insights into further optimization of 3-methylene-2-oxoindoline-5-carboxamide derivatives for the discovery of more potent RAF/MEK/ERK pathway regulators as anti-lung cancer agents.

Keywords 2-Oxoindoline-5-carboxamide · Synthesis · Molecular docking · Lung cancer · RAF/MEK/ERK pathway

Introduction

Deregulation of signaling pathways have been implicated to promote carcinogenesis. The Ras signaling pathway occurs downstream of most growth factor's binding to their receptors and is an essential signal transduction cascade that controls cell survival, growth, differentiation and transformation (Downward 2003; Schubert et al. 2007). The RAF/MEK/ERK pathway represents one of the best-characterized Ras pathways, which promotes cell cycle progression and cell proliferation (Abdel-Rahman 2016; Martinelli et al. 2017). Substantial evidence has supported that deregulation of this pathway with downstream effectors ERK1/2 constitutively active is involved in the oncogenesis of various human cancers. About 30% of lung adenocarcinomas contain KRAS mutations (Pao et al. 2005), and BRAF mutations exist in about 66% of malignant melanomas (Davies et al. 2002). This pathway is also activated to various degrees in many other malignant tumor, such as thyroid cancer (Espinosa et al. 2007), colorectal cancer (Douillard et al. 2013), which lead to excessive activation of MEK1/2 and then ERK1/2. Therefore, RAF/MEK/ERK signaling cascade has being treated as an important target for anti-cancer drug discovery (Roberts and Der 2007).

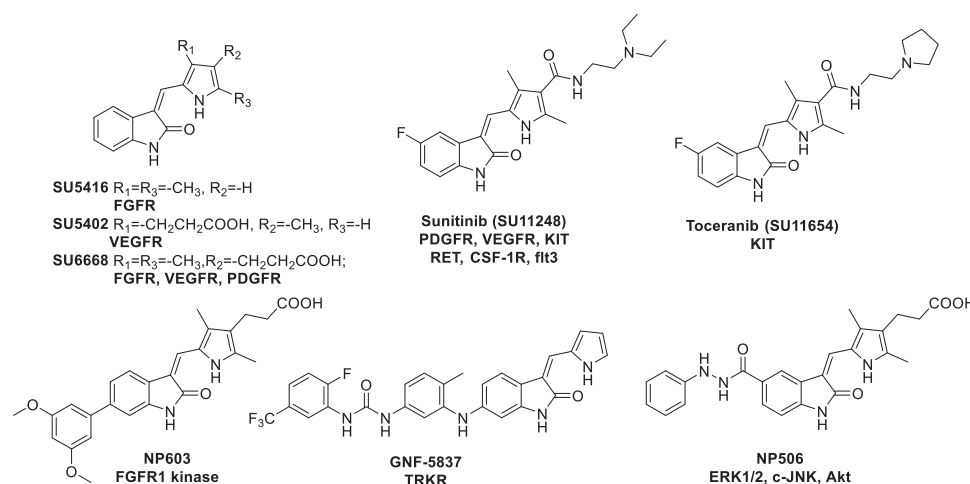
3-(1*H*-pyrrol-2-yl) methylene-indolin-2-one analogs have been widely applied in the development of anti-cancer agents (Fig. 1). SU5416, SU5402 have been shown to be specific inhibitors of the kinase activity of the fibroblast growth factor receptor (FGFR) and vascular endothelial growth factor receptor (VEGFR), respectively, whereas SU6668 showed inhibitory activity against multi tyrosine kinase, such as FGFR, VEGFR, and platelet-derived growth factor (PDGFR) (Sun et al. 1998, 1999). Sunitinib (SU11248) and toceranib (SU11654) are applied for the treatment of renal cell carcinoma and imatinib-resistant

✉ Qianbin Li
qbli@csu.edu.cn

¹ Department of Medicinal Chemistry, Xiangya School of Pharmaceutical Sciences, Central South University, 410013 Changsha, Hunan, China

² Department of Pharmacology, Xiangya School of Pharmaceutical Sciences, Central South University, 410013 Changsha, Hunan, China

Fig. 1 Kinase inhibitors with 3-(1*H*-pyrrol-2-yl)methylene-indolin-2-one scaffold



gastrointestinal stromal tumor, respectively, because of their broad inhibition against multi-tyrosine kinases, such as PDGFR, VEGFR, KIT, RET, CSF-1R, and FLT3 (Gan et al. 2009).

C5 or C6-substituted indolin-2-one derivatives are also widely applied in the development of anticancer agents, especially for Ser/Thr kinase inhibitors. NP603 was discovered as a novel and potent inhibitor of FGFR1 tyrosine kinase (Kammasud et al. 2007). GNF-5837, a potent, selective, and orally bioavailable pan-TRKR inhibitor with large substituent on C6 position resulted in the inhibition of MEK/ERK pathway (Albaugh et al. 2012). NP506, an analog of NP603, inhibited the activation of ERK, c-Jun-N-terminal-kinase (JNK) and AKT after the rhFGF-2 stimulation other than the tyrosine phosphorylation in FGFR, VEGFR, and PDGFR. The introduction of the arylhydrazide motif on C5 position of the indolin-2-one scaffold led to the inhibitory effect of ERK and JNK activation (Kammasud et al. 2009).

Herein, to find modulators of MEK/ERK pathway, 5-carboxyl-indolin-2-one derivatives, 3-(1*H*-furan-2-yl)methylene-2-oxindoline-5-carboxamide and 3-(1*H*-pyrrol-2-yl)methylene-2-oxindoline-5-carboxamide are designed (Fig. 2) and synthesized based on our previous works (Li et al. 2009, 2010). The target compounds were biologically evaluated in A549 human lung adenocarcinoma epithelial cell for the inhibition of cell proliferation. Structure–activity relationship was also studied for part I and II. Western blot analysis was applied to preliminarily demonstrate the influence of active compounds on the components of RAF/MEK/ERK pathway, such as phospho-ERK1/2 level, which is the substrate of dual-phosphorylation kinase MEK1/2. Finally, the molecular modeling studies were conformed to figure out the binding mode of active compound to the possible kinases of RAF/MEK/ERK pathway.

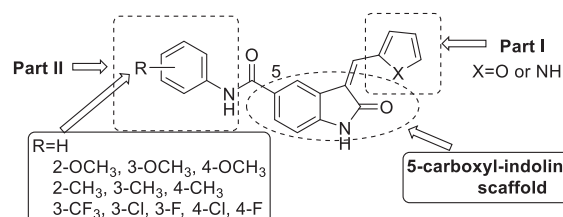


Fig. 2 Design strategies for 3-methylene-2-oxindoline-5-carboxamide derivatives

Materials and methods

Chemistry

All reagents and solvents were obtained from commercial suppliers and used as received unless otherwise stated. Reactions were monitored by thin layer chromatography with 0.25 mm pre-coated silica gel plates (60GF-254) and visualized with ultraviolet (UV) light at 254 nm, iodine stain or by KMnO_4 . Flash column chromatography was performed on silica gel (200–300 mesh) using solvents as indicated. Melting points were determined uncorrected on Boetius apparatus. ^1H -nuclear magnetic resonance (NMR) and ^{13}C -NMR spectra were recorded at 300 MHz (^1H) and at 75 MHz (^{13}C) spectrometers (Bruker, Germany). The measurements were made in dimethyl sulfoxide (DMSO)- d_6 solutions, δ in parts per million and J in hertz, using tetramethylsilane as an internal standard. High resolution mass spectra (HRMS) were recorded on MALDI-TOF/TOF-MS spectrometer (Bruker, Germany). The purity of compounds was determined on a Shimadzu LC-20AT HPLC instrument using a Promosil C18 column (5 μm , 250 \times 4.6 mm) with UV detection (254 nm), eluted with 70% methanol/30% water over 20 min and a flow rate of 1.0 mL/min.

2-Oxoindoline-5-carboxylic acid (**4**)

To a solution of trichloroacetic aldehyde (9.0 g, 61 mmol) in 120 mL of water were added anhydrous sodium sulfate (65 g, 458 mmol), 4-aminobenzoic acid (6.9 g, 51 mmol) and 4.3 mL of hydrochloric acid in 30 mL of water. Hydroxylamine hydrochloride (10.8 g, 152 mmol) in 50 mL of water was added drop wise to the mixture mentioned above. The resulting mixture was heated to 60–70 °C and kept stirring for 2 h. The precipitate formed was collected by filtration, washed with water and dried under vacuum. 14.8 g of intermediate compound **2** was obtained as a light yellow solid and was applied to the next reaction without any purification.

To 32.6 mL of concentrated sulfuric acid at 60–70 °C was added compound **2** (9.2 g, 44 mmol) in portions. The mixture was then heated at 80 °C for 20 min and cooled to room temperature, which was poured into 100 mL of ice-water with stirring for 1 h. The precipitate was filtrated, washed to neutral with water and added water (25 mL) and 80% hydrazine hydrate (25 mL, 62 mmol). The mixture was then heated to 140 °C and kept stirring for 6 h. After cooling to room temperature, the pH of the mixture was adjusted to 2 with hydrochloric acid, which yielded 8.0 g of 2-oxoindoline-5-carboxylic acid (**4**) as a light yellow solid. Mp >300 °C (Ogawa et al. 1988).

General procedure for the synthesis of compounds **6** and **7**

To a solution of **4** (1.77 g, 10 mmol) in 120 mL of dichloromethane and 10 mL of DMF was added 4-methylmorpholine or DIEA (10 mL), TBTU (4.81 g, 15 mmol) and aniline derivatives (11 mmol). The mixture was stirred under room temperature for 18 h and washed in turn with 5% sodium carbonate solution, 5% citric acid solution and saturated sodium chloride solution. After dried by anhydrous sodium sulfate, the organic layer was evaporated to dryness. The residue was purified with flash chromatography (CH₂Cl₂:CH₃OH, 50:1) to afford intermediates **5a–5l**, which were used in the next step in short time. To a solution of compounds **5a–5l** (1.0 mmol) in 10 mL methanol was added piperidine (30 μL) and 1*H*-pyrrole-2-carbaldehyde/furan-2-carbaldehyde (1.0 mmol). The mixture was stirred at 60 °C for 5 h and cooled to room temperature. After kept in fridge overnight, the target compounds **6a–6l** and **7a–7l** were obtained in high yields.

3-((1*H*-pyrrol-2-yl)methylene)-2-oxo-*N*-phenylindoline-5-carboxamide (**6a**) Yield 83.3%, yellow crystals, mp >300 °C. ¹H-NMR (300 MHz, DMSO-*d*₆) δ: 6.40 (s, 1H, Ar-H), 6.94–7.12 (m, 3H, Ar-H), 7.34–7.42 (m, 3H, Ar-H), 7.78–7.86 (m, 3H, Ar-H), 7.89 (s, 1H, =CH), 8.28 (s, 1H, Ar-H), 10.10 (s, 1H, NH), 11.21 (s, 1H, NH), 13.27 (s, 1H,

NH). ¹³C-NMR (75 MHz, DMSO-*d*₆) δ: 109.0, 111.7, 115.8, 118.0, 120.0, 120.2, 121.1, 123.3, 125.0, 125.7, 127.0, 127.3, 128.0, 128.5, 128.5, 129.5, 139.4, 141.4, 165.5 (C=O), 169.5 (C=O). HRMS: *m/z* 330.1236 [M + H]⁺ (calcd 330.1243).

3-((1*H*-pyrrol-2-yl)methylene)-*N*-(2-methoxyphenyl)-2-oxoindoline-5-carboxamide (**6b**) Yield 81%, yellow crystals, mp: 232.1–234.2 °C. ¹H-NMR (300 MHz, DMSO-*d*₆) δ: 3.86 (s, 3H, –CH₃), 6.40 (s, 1H, Ar-H), 6.91–7.01 (m, 3H, Ar-H), 7.01–7.17 (m, 2H, Ar-H), 7.41 (s, 1H, Ar-H), 7.81 (d, 2H, Ar-H, *J* = 8.1 Hz), 7.90 (s, 1H, =CH), 8.30 (s, 1H, Ar-H), 9.26 (s, 1H, NH), 11.20 (s, 1H, NH), 13.26 (s, 1H, NH). ¹³C-NMR (75 MHz, DMSO-*d*₆) δ: 56.2 (–OCH₃), 109.6, 111.8, 112.2, 116.3, 118.4, 121.0, 121.6, 124.5, 125.7, 125.8, 126.9, 127.2, 127.6, 127.7, 128.1, 130.0, 142.0, 151.7, 165.5 (C=O), 170.0 (C=O). HRMS: *m/z* 360.1348 [M + H]⁺ (calcd 360.1348).

3-((1*H*-pyrrol-2-yl)methylene)-*N*-(3-methoxyphenyl)-2-oxoindoline-5-carboxamide (**6c**) Yield 71%, yellow crystals, mp: 228.1–230.2 °C. ¹H-NMR (300 MHz, DMSO-*d*₆) δ: 3.77 (s, 3H, –CH₃), 6.39 (s, 1H, Ar-H), 6.54 (d, 1H, Ar-H, *J* = 8.3 Hz), 6.93 (s, 1H, Ar-H), 6.99–7.02 (d, *J* = 8.1 Hz, 1H, Ar-H), 7.22–7.28 (m, 1H, Ar-H), 7.38–7.40 (m, 2H, Ar-H), 7.48 (s, 1H, Ar-H), 7.79–7.81 (m, 1H, Ar-H), 7.89 (s, 1H, =CH), 8.26 (s, 1H, Ar-H), 10.11 (s, 1H, NH), 11.21 (s, 1H, NH), 13.26 (s, 1H, NH). ¹³C-NMR (75 MHz, DMSO-*d*₆) δ: 55.0 (–OCH₃), 105.9, 108.8, 109.0, 111.7, 112.4, 115.8, 118.0, 121.1, 125.0, 126.4, 126.7, 127.3, 128.0, 129.3, 129.5, 140.6, 141.4, 159.4, 165.6 (C=O), 169.5 (C=O). HRMS: *m/z* 360.1348 [M + H]⁺ (calcd 360.1348).

3-((1*H*-pyrrol-2-yl)methylene)-*N*-(4-methoxyphenyl)-2-oxoindoline-5-carboxamide (**6d**) Yield 92.0%, yellow crystals, mp >300 °C. ¹H-NMR (300 MHz, DMSO-*d*₆) δ: 3.79 (s, 3H, –CH₃), 6.40 (s, 1H, Ar-H), 6.93 (s, 1H, Ar-H), 7.00 (d, *J* = 8.1 Hz, 1H, Ar-H), 7.19 (m, 2H, Ar-H), 7.41 (s, 1H, Ar-H), 7.79–7.85 (m, 3H, Ar-H), 7.88 (s, 1H, =CH), 8.26 (s, 1H, Ar-H), 10.18 (s, 1H, NH), 11.20 (s, 1H, NH), 13.26 (s, 1H, NH). ¹³C-NMR (75 MHz, DMSO-*d*₆) δ: 55.8 (–OCH₃), 109.5, 112.2, 115.5, 115.8, 116.3, 118.5, 121.7, 122.4, 122.5, 125.5, 126.9, 127.4, 127.8, 128.4, 130.0, 136.3, 136.3, 142.0, 166.0 (C=O), 170.0 (C=O). HRMS: *m/z* 360.1346 [M + H]⁺ (calcd 360.1348).

3-((1*H*-pyrrol-2-yl)methylene)-2-oxo-*N*-2-tolylindoline-5-carboxamide (**6e**) Yield 78.0%, yellow crystals, mp 275.1–277.8 °C. ¹H-NMR (300 MHz, DMSO-*d*₆) δ: 2.22 (s, 3H, –CH₃), 6.38 (d, *J* = 3.39 Hz, 1H, Ar-H), 6.92 (s, 1H, Ar-H), 7.01 (d, 1H, Ar-H, *J* = 2.46 Hz), 7.14–7.41 (m, 5H, Ar-H), 7.82–7.86 (m, 2H, Ar-H), 8.30 (s, 1H, Ar-H), 9.75

(s, 1H, NH), 11.20 (s, 1H, NH), 13.27 (s, 1H, NH). ^{13}C -NMR (75 MHz, DMSO- d_6) δ : 18.5 (–CH $_3$), 109.5, 112.2, 116.4, 118.5, 121.6, 125.5, 126.2, 126.4, 126.8, 127.0, 127.4, 127.7, 128.2, 130.0, 130.8, 134.1, 137.2, 141.9, 165.8 (C=O), 170.0 (C=O). HRMS: m/z 344.1396 [M + H] $^+$ (calcd 344.1399).

3-((1*H*-pyrrol-2-yl)methylene)-2-oxo-*N*-3-tolyindoline-5-carboxamide (**6f**) Yield 80.2%, yellow crystals, mp 273.0–274.0 °C. ^1H -NMR (300 MHz, DMSO- d_6) δ : 2.32 (s, 3H, –CH $_3$), 6.39–6.40 (d, 1H, Ar–H, J = 3.6 Hz), 6.90–6.93 (m, 2H, Ar–H), 6.99 (d, 1H, Ar–H, J = 8.0 Hz), 7.24 (t, 1H, Ar–H, J = 7.8 Hz), 7.41 (s, 1H, Ar–H), 7.60 (m, 2H, Ar–H), 7.79–7.82 (d, J = 8.4 Hz, 1H, Ar–H), 7.87 (s, 1H, =CH), 8.27 (s, 1H, Ar–H), 10.04 (s, 1H, NH), 11.20 (s, 1H, NH), 13.27 (s, 1H, NH). ^{13}C -NMR (75 MHz, DMSO- d_6) δ : 19.6 (–CH $_3$), 109.5, 112.2, 116.3, 117.7, 121.4, 123.2, 125.5, 126.5, 127.8, 128.8, 129.0, 130.0, 134.4, 135.7, 137.8, 138.9, 140.8, 149.9, 164.6 (C=O), 169.8 (C=O). HRMS: m/z 344.1393 [M + H] $^+$ (calcd 344.1399).

3-((1*H*-pyrrol-2-yl)methylene)-2-oxo-*N*-4-tolyindoline-5-carboxamide (**6g**) Yield 75%, yellow crystals, mp >300 °C. ^1H -NMR (300 MHz, DMSO- d_6) δ : 2.29 (s, 3H, –CH $_3$), 6.39 (s, 1H, Ar–H), 6.93 (s, 1H, Ar–H), 7.00 (d, J = 8.0 Hz, 1H, Ar–H), 7.16 (d, J = 8.4 Hz, 2H, Ar–H), 7.42 (s, 1H, Ar–H), 7.67 (d, J = 8.4 Hz, 2H, Ar–H), 7.80 (d, 1H, Ar–H, J = 8.0 Hz), 7.88 (s, 1H, =CH), 8.27 (s, 1H, Ar–H), 10.06 (s, 1H, NH), 11.22 (s, 1H, NH), 13.27 (s, 1H, NH). ^{13}C -NMR (75 MHz, DMSO- d_6) δ : 20.8 (–CH $_3$), 109.4, 112.1, 116.2, 118.3, 120.6 (2C), 121.5, 125.3, 126.7, 127.3, 127.6, 128.4, 129.3 (2C), 129.8, 132.6, 137.2, 141.7, 165.7 (C=O), 169.9 (C=O). HRMS: m/z 344.1371 [M + H] $^+$ (calcd 344.1399).

3-((1*H*-pyrrol-2-yl)methylene)-2-oxo-*N*-(3-(trifluoromethyl)phenyl)indoline-5-carboxamide (**6h**) Yield 71.5%, yellow crystals, mp 258.1–260.2 °C. ^1H -NMR (300 MHz, DMSO- d_6) δ : 6.40 (s, 1H, Ar–H), 6.94 (s, 1H, Ar–H), 7.02–7.04 (d, J = 8.2 Hz, 1H, Ar–H), 7.43–7.46 (m, 2H, Ar–H), 7.59–7.64 (m, 1H, Ar–H), 7.82–7.90 (m, 2H, Ar–H), 8.09–8.12 (d, J = 8.3 Hz, 1H, Ar–H), 8.25–8.30 (m, 2H, Ar–H), 10.45 (s, 1H, NH), 11.25 (s, 1H, NH), 13.27 (s, 1H, NH). ^{13}C -NMR (75 MHz, DMSO- d_6) δ : 109.1, 111.8, 115.7, 116.2, 118.0, 119.6, 121.2, 123.6, 125.0, 126.5, 127.1, 127.3, 127.4, 129.1, 129.5, 129.5, 129.8, 140.2, 141.7, 165.9 (C=O), 169.5 (C=O). HRMS: m/z 398.1089 [M + H] $^+$ (calcd 398.1116).

3-((1*H*-pyrrol-2-yl)methylene)-*N*-(3-chlorophenyl)-2-oxoindoline-5-carboxamide (**6i**) Yield 84%, yellow crystals, mp 257.0–259.7 °C. ^1H -NMR (300 MHz, DMSO- d_6) δ : 6.40 (s, 1H, Ar–H), 6.93 (s, 1H, Ar–H), 7.01 (d, J = 8.1 Hz, 1H, Ar–H), 7.16 (d, J = 7.1 Hz, 1H, Ar–H), 7.36–7.42

(m, 2H, Ar–H), 7.72–7.85 (m, 2H, Ar–H), 7.89 (s, 1H, =CH), 7.98 (s, 1H, Ar–H), 8.26 (s, 1H, Ar–H), 10.29 (s, 1H, NH), 11.23 (s, 1H, NH), 13.26 (s, 1H, NH). ^{13}C -NMR (75 MHz, DMSO- d_6) δ : 109.6, 112.3, 116.2, 118.5, 118.9, 120.0, 121.7, 123.5, 125.5, 127.0, 127.6, 127.8, 128.1, 130.0, 130.8, 133.4, 141.4, 142.2, 166.3 (C=O), 170.0 (C=O). HRMS: m/z 364.0846 [M + H] $^+$ (calcd 364.0853).

3-((1*H*-pyrrol-2-yl)methylene)-*N*-(4-chlorophenyl)-2-oxoindoline-5-carboxamide (**6j**) Yield 86%, yellow crystals, mp >300 °C. ^1H -NMR (300 MHz, DMSO- d_6) δ : 6.40 (s, 1H, Ar–H), 6.94–7.02 (m, 2H, Ar–H), 7.38–7.43 (m, 3H, Ar–H), 7.79–7.85 (m, 3H, Ar–H), 7.89 (s, 1H, =CH), 8.26 (s, 1H, Ar–H), 10.19 (s, 1H, NH), 11.21 (s, 1H, NH), 13.25 (s, 1H, NH). ^{13}C -NMR (75 MHz, DMSO- d_6) δ : 109.6, 112.2, 116.3, 118.5, 121.7, 122.2 (2C), 125.5, 126.9, 127.4, 127.5, 127.8, 128.2, 129.0 (2C), 130.0, 138.9, 142.1, 166.2 (C=O), 170.0 (C=O). HRMS: m/z 364.0853 [M + H] $^+$ (calcd 364.0853).

3-((1*H*-pyrrol-2-yl)methylene)-*N*-(3-fluorophenyl)-2-oxoindoline-5-carboxamide (**6k**) Yield 75%, yellow crystals, mp: 278.0–280.0 °C. ^1H -NMR (300 MHz, DMSO- d_6) δ : 6.40 (s, 1H, Ar–H), 6.90–6.94 (m, 2H, Ar–H), 7.01 (d, J = 8.1 Hz, 1H, Ar–H), 7.36–7.42 (m, 2H, Ar–H), 7.56–7.59 (m, 1H, Ar–H), 7.75–7.82 (m, 2H, Ar–H), 7.90 (s, 1H, =CH), 8.26 (s, 1H, Ar–H), 10.33 (s, 1H, NH), 11.24 (s, 1H, NH), 13.26 (s, 1H, NH). ^{13}C -NMR (75 MHz, DMSO- d_6) δ : 106.9, 109.1, 109.6, 111.8, 115.8, 115.8, 118.1, 121.2, 125.0, 126.5, 127.0, 127.5, 127.6, 129.5, 130.2, 141.3, 141.6, 163.7, 165.8 (C=O), 169.5 (C=O). HRMS: m/z 348.1156 [M + H] $^+$ (calcd 348.1148).

3-((1*H*-pyrrol-2-yl)methylene)-*N*-(4-fluorophenyl)-2-oxoindoline-5-carboxamide (**6l**) Yield 76.7%, yellow crystals, mp >300 °C. ^1H -NMR (300 MHz, DMSO- d_6) δ : 6.40 (s, 1H, Ar–H), 6.93–7.02 (m, 2H, Ar–H), 7.20 (s, 2H, Ar–H), 7.42 (s, 1H, Ar–H), 7.69–7.81 (m, 3H, Ar–H), 7.89 (s, 1H, =CH), 8.26 (s, 1H, Ar–H), 10.20 (s, 1H, NH), 11.22 (s, 1H, NH), 13.26 (s, 1H, NH). ^{13}C -NMR (75 MHz, DMSO- d_6) δ : 109.0, 111.7, 115.0, 115.3, 115.8, 118.0, 121.2, 121.9, 122.0, 125.0, 126.4, 126.9, 127.3, 127.8, 129.5, 135.8, 141.5, 156.5, 165.5 (C=O), 169.5 (C=O). HRMS: m/z 348.1140 [M + H] $^+$ (calcd 348.1148).

3-(Furan-2-ylmethylene)-2-oxo-*N*-phenylindoline-5-carboxamide (**7a**) Yield 79.2%, yellow crystals, mp 300.6–301.1 °C. ^1H -NMR (300 MHz, DMSO- d_6) δ : 6.83–6.85 (m, 1H, Ar–H), 6.99 (d, J = 8.1 Hz, 1H, Ar–H), 7.07–7.12 (m, 1H, Ar–H), 7.33–7.38 (m, 3H, Ar–H), 7.44 (s, 1H, Ar–H), 7.79 (d, J = 8.0 Hz, 2H, Ar–H), 7.90 (d, J = 8.1 Hz, 1H, Ar–H), 8.19 (s, 1H, =CH), 8.92 (s, 1H, Ar–H), 10.25 (s, 1H, NH), 10.91 (s, 1H, NH). ^{13}C -NMR (75 MHz,

DMSO- d_6) δ : 109.0, 113.7, 120.2 (2C), 120.3, 121.1, 121.4, 121.6, 123.3, 124.4, 128.4, 128.5 (2C), 129.5, 139.5, 145.1, 147.6, 150.5, 165.7 (C=O), 169.5 (C=O). HRMS: m/z 331.1082 [M + H]⁺ (calcd 331.1083).

3-(Furan-2-ylmethylene)-N-(2-methoxyphenyl)-2-oxoindoline-5-carboxamide (**7b**) Yield 75.4%, yellow crystals, mp 268.2–271.1 °C. ¹H-NMR (300 MHz, DMSO- d_6) δ : 3.87 (s, 3H, –CH₃), 6.86 (s, 1H, Ar–H), 6.96–7.00 (m, 2H, Ar–H), 7.10–7.17 (m, 2H, Ar–H), 7.35 (s, 1H, Ar–H), 7.44 (s, 1H, Ar–H), 7.90–7.94 (m, 2H, Ar–H), 8.14 (s, 1H, =CH), 8.93 (s, 1H, Ar–H), 9.32 (s, 1H, NH), 10.92 (s, 1H, NH). ¹³C-NMR (75 MHz, DMSO- d_6) δ : 55.9 (–OCH₃), 109.2, 111.3, 113.8, 120.2, 120.4, 121.2, 121.4, 121.6, 123.1, 123.9, 125.0, 127.3, 127.8, 129.3, 145.2, 147.4, 150.6, 150.8, 164.9 (C=O), 169.5 (C=O). HRMS: m/z 361.1189 [M + H]⁺ (calcd 361.1188).

3-(Furan-2-ylmethylene)-N-(3-methoxyphenyl)-2-oxoindoline-5-carboxamide (**7c**) Yield 68.8%, yellow crystals, mp 246.2–247.3 °C. ¹H-NMR (300 MHz, DMSO- d_6) δ : 3.76 (s, 3H, –CH₃), 6.66–6.69 (m, 1H, Ar–H), 6.84 (s, 1H, Ar–H), 6.97–7.00 (d, J = 7.7 Hz, 1H, Ar–H), 7.22–7.27 (m, 1H, Ar–H), 7.35–7.49 (m, 4H, Ar–H), 7.88–7.90 (m, 1H, Ar–H), 8.19 (s, 1H, =CH), 8.91 (s, 1H, Ar–H), 10.20 (s, 1H, NH), 10.90 (s, 1H, NH). ¹³C-NMR (75 MHz, DMSO- d_6) δ : 55.0 (–OCH₃), 106.0, 108.8, 109.0, 112.5, 113.8, 120.4, 121.1, 121.3, 121.6, 124.3, 128.4, 129.3, 129.5, 140.6, 145.1, 147.7, 150.5, 159.4, 165.7 (C=O), 169.5 (C=O). HRMS: m/z 361.1176 [M + H]⁺ (calcd 361.1188).

3-(Furan-2-ylmethylene)-N-(4-methoxyphenyl)-2-oxoindoline-5-carboxamide (**7d**) Yield 73%, yellow crystals, mp 309.0–310.0 °C. ¹H-NMR (300 MHz, DMSO- d_6) δ : 3.75 (s, 3H, –CH₃), 6.84 (s, 1H, Ar–H), 6.92–6.99 (m, 3H, Ar–H), 7.35 (s, 1H, Ar–H), 7.43 (s, 1H, Ar–H), 7.68–7.71 (m, 2H, Ar–H), 7.88 (s, 1H, Ar–H), 8.19 (s, 1H, =CH), 8.91 (s, 1H, Ar–H), 10.12 (s, 1H, NH), 10.90 (s, 1H, NH). ¹³C-NMR (75 MHz, DMSO- d_6) δ : 55.2 (–OCH₃), 109.0, 113.6 (2C), 113.7, 120.3, 121.1, 121.4, 121.6, 121.9 (2C), 124.3, 128.5, 129.3, 132.5, 145.0, 147.6, 150.5, 155.4, 165.3 (C=O), 169.5 (C=O). HRMS: m/z 361.1184 [M + H]⁺ (calcd 361.1188).

3-(Furan-2-ylmethylene)-2-oxo-N-2-tolyindoline-5-carboxamide (**7e**) Yield 80%, yellow crystals, mp 286.5–288.3 °C. ¹H-NMR (300 MHz, DMSO- d_6) δ : 2.30 (s, 3H, –CH₃), 6.83 (s, 1H, Ar–H), 6.98 (d, J = 6.6 Hz, 1H, Ar–H), 7.26–7.34 (m, 3H, Ar–H), 7.35 (s, 1H, Ar–H), 7.42–7.43 (m, 2H, Ar–H), 7.90 (s, 1H, Ar–H), 8.11 (s, 1H, =CH), 8.94 (s, 1H, Ar–H), 9.80 (s, 1H, NH), 10.89 (s, 1H, NH). ¹³C-NMR (75 MHz, DMSO- d_6) δ : 18.4 (–CH₃), 109.6, 114.3, 120.8, 121.6, 121.9, 122.0, 124.8, 126.1,

126.4, 126.8, 128.6, 130.0, 130.8, 133.8, 137.2, 145.6, 148.0, 151.1, 166.0 (C=O), 170.0 (C=O). HRMS: m/z 345.1242 [M + H]⁺ (calcd 345.1239).

3-(Furan-2-ylmethylene)-2-oxo-N-3-tolyindoline-5-carboxamide (**7f**) Yield 81%, yellow crystals, mp 274.8–278.0 °C. ¹H-NMR (300 MHz, DMSO- d_6) δ : 2.32 (s, 3H, –CH₃), 6.83–7.00 (m, 3H, Ar–H), 7.20–7.25 (m, 1H, Ar–H), 7.35 (s, 1H, Ar–H), 7.43 (s, 1H, Ar–H), 7.55–7.66 (m, 1H, Ar–H), 7.89 (s, 1H, Ar–H), 7.92 (s, 1H, Ar–H), 8.19 (s, 1H, =CH), 8.92 (s, 1H, Ar–H), 10.14 (s, 1H, NH), 10.89 (s, 1H, NH). ¹³C-NMR (75 MHz, DMSO- d_6) δ : 21.7 (–CH₃), 109.4, 114.3, 118.0, 120.8, 121.3, 121.6, 121.9, 122.1, 124.5, 124.9, 128.8, 128.9, 129.9, 138.1, 139.9, 145.6, 148.1, 151.0, 166.1 (C=O), 170.0 (C=O). HRMS: m/z 345.1236 [M + H]⁺ (calcd 345.1239).

3-(Furan-2-ylmethylene)-2-oxo-N-4-tolyindoline-5-carboxamide (**7g**) Yield 90%, yellow crystals, mp 292.0–294.0 °C. ¹H-NMR (300 MHz, DMSO- d_6) δ : 2.29 (s, 3H, –CH₃), 6.83–6.85 (m, 1H, Ar–H), 6.98 (d, J = 8.1 Hz, 1H, Ar–H), 7.15 (d, J = 8.3 Hz, 2H, Ar–H), 7.35 (s, 1H, Ar–H), 7.44 (s, 1H, Ar–H), 7.68 (d, J = 8.3 Hz, 2H, Ar–H), 7.90 (d, J = 8.1 Hz, 1H, Ar–H), 8.18 (s, 1H, =CH), 8.91 (s, 1H, Ar–H), 10.17 (s, 1H, NH), 10.91 (s, 1H, NH). ¹³C-NMR (75 MHz, DMSO- d_6) δ : 20.5 (–CH₃), 108.9, 113.7, 120.3 (2C), 121.1, 121.4, 121.6, 124.4, 128.5, 128.9 (2C), 129.4, 132.2, 133.0, 136.9, 145.0, 147.6, 150.5, 165.5 (C=O), 169.5 (C=O). HRMS: m/z 345.1238 [M + H]⁺ (calcd 345.1239).

3-(Furan-2-ylmethylene)-2-oxo-N-(3-(trifluoromethyl)phenyl)indoline-5-carboxamide (**7h**) Yield 72%, yellow crystals, mp 275.0–276.7 °C. ¹H-NMR (300 MHz, DMSO- d_6) δ : 6.84 (s, 1H, Ar–H), 7.01 (d, J = 8.1 Hz, 1H, Ar–H), 7.35 (s, 1H, Ar–H), 7.45 (s, 2H, Ar–H), 7.57–7.60 (m, 1H, Ar–H), 7.94 (d, J = 8.1 Hz, 1H, Ar–H), 8.03 (d, J = 7.9 Hz, 1H, Ar–H), 8.22 (s, 1H, =CH), 8.31 (s, 1H, Ar–H), 8.95 (s, 1H, Ar–H), 10.55 (s, 1H, NH), 10.94 (s, 1H, NH). ¹³C-NMR (75 MHz, DMSO- d_6) δ : 109.6, 114.3, 116.7, 120.1, 121.0, 121.7, 121.7, 122.3, 124.2, 124.9, 128.2, 129.7, 129.9, 130.1, 130.3, 140.8, 145.9, 148.3, 151.0, 166.6 (C=O), 170.0 (C=O). HRMS: m/z 399.0956 [M + H]⁺ (calcd 399.0957).

N-(3-chlorophenyl)-3-(furan-2-ylmethylene)-2-oxoindoline-5-carboxamide (**7i**) Yield 74%, yellow crystals, mp 274.0–276.2 °C. ¹H-NMR (300 MHz, DMSO- d_6) δ : 6.84–6.85 (m, 1H, Ar–H), 7.00 (d, J = 7.9 Hz, 1H, Ar–H), 7.15 (d, J = 8.1 Hz, 1H, Ar–H), 7.36–7.42 (m, 2H, Ar–H), 7.45 (s, 1H, Ar–H), 7.70 (d, J = 8.1 Hz, 1H, Ar–H), 7.91 (d, J = 7.9 Hz, 1H, Ar–H), 8.03 (s, 1H, Ar–H), 8.21 (s, 1H, =CH), 8.93 (s, 1H, Ar–H), 10.42 (s, 1H, NH), 10.95 (s, 1H,

NH). ^{13}C -NMR (75 MHz, DMSO- d_6) δ : 109.0, 113.8, 118.6, 119.6 (2C), 120.5, 121.2, 121.7, 123.0, 124.4, 127.9, 129.5, 130.2 (2C), 132.9, 145.4, 147.7, 150.5, 165.9 (C=O), 169.5 (C=O). HRMS: m/z 365.0689 $[\text{M} + \text{H}]^+$ (calcd 365.0693).

N-(4-chlorophenyl)-3-(furan-2-ylmethylene)-2-oxoindoline-5-carboxamide (**7j**) Yield 87%, yellow crystals, mp >300 °C. ^1H -NMR (300 MHz, DMSO- d_6) δ : 6.83–6.85 (m, 1H, Ar-H), 6.99 (d, $J = 8.1$ Hz, 1H, Ar-H), 7.34–7.44 (m, 4H, Ar-H), 7.81–7.92 (m, 3H, Ar-H), 8.19 (s, 1H, =CH), 8.92 (s, 1H, Ar-H), 10.37 (s, 1H, NH), 10.91 (s, 1H, NH). ^{13}C -NMR (75 MHz, DMSO- d_6) δ : 109.5, 114.3, 120.9, 121.7, 121.8, 122.2 (2C), 124.9, 127.4, 128.5, 128.9 (2C), 129.4, 130.0, 138.9, 145.8, 148.2, 151.0, 166.3 (C=O), 170.0 (C=O). HRMS: m/z 365.0687 $[\text{M} + \text{H}]^+$ (calcd 365.0693).

N-(3-fluorophenyl)-3-(furan-2-ylmethylene)-2-oxoindoline-5-carboxamide (**7k**) Yield 80%, yellow crystals, mp: >300 °C. ^1H -NMR (300 MHz, DMSO- d_6) δ : 6.84 (s, 1H, Ar-H), 6.89–6.95 (m, 1H, Ar-H), 6.99–7.02 (m, 1H, Ar-H), 7.35–7.45 (m, 3H, Ar-H), 7.57–7.77 (m, 1H, Ar-H), 7.81–7.90 (m, 1H, Ar-H), 7.92–7.93 (m, 1H, Ar-H), 8.20 (s, 1H, =CH), 8.93 (s, 1H, Ar-H), 10.44 (s, 1H, NH), 10.93 (s, 1H, NH). ^{13}C -NMR (75 MHz, DMSO- d_6) δ : 109.0, 113.8, 115.9, 120.4, 121.1, 121.2, 121.7, 124.4, 127.9, 129.5, 130.1, 130.2, 141.2, 141.3, 145.3, 147.7, 150.5, 163.6, 165.9 (C=O), 169.5 (C=O). HRMS: m/z 349.0969 $[\text{M} + \text{H}]^+$ (calcd 349.0988).

N-(4-fluorophenyl)-3-(furan-2-ylmethylene)-2-oxoindoline-5-carboxamide (**7l**) Yield 76%, yellow crystals, mp: >300 °C. ^1H -NMR (300 MHz, DMSO- d_6) δ : 6.84 (s, 1H, Ar-H), 6.89–7.00 (m, 1H, Ar-H), 7.13–7.22 (m, 2H, Ar-H), 7.35 (s, 1H, Ar-H), 7.44 (s, 1H, Ar-H), 7.81–7.91 (m, 3H, Ar-H), 8.19 (s, 1H, =CH), 8.92 (s, 1H, Ar-H), 10.29 (s, 1H, NH), 10.90 (s, 1H, NH). ^{13}C -NMR (75 MHz, DMSO- d_6) δ : 109.0, 113.7, 114.9, 115.3, 120.4, 121.1, 121.3, 121.7, 121.9, 122.0, 122.1, 124.3, 128.2, 129.4, 135.8, 145.1, 147.7, 150.5, 165.6 (C=O), 169.5 (C=O). HRMS: m/z 349.0973 $[\text{M} + \text{H}]^+$ (calcd 349.0988).

Biology

Human lung adenocarcinoma epithelial A549 cells were obtained from American Type Culture Collection. A549 cells were cultured in RPMI-1640 medium supplemented with 10% (v/v) of heat-inactivated fetal bovine calf serum at 37 °C in a fully humidified atmosphere (5% CO_2). All experiments were performed on logarithmically growing cells. The MEK inhibitor selumetinib was purchased from

Selleck China. All reagents were prepared and used as recommended by their suppliers.

Cell proliferation assays

A549 cells were seeded at a density of 1×10^5 cells (100 μL per well) in 96-well plates and pretreated with active compounds (0, 0.3, 1, 3, 10, 30, and 100 μM) for 48 h at 37 °C in a fully humidified atmosphere containing 5% CO_2 , with cisplatin and sunitinib as positive control (Xu et al. 2016). Upon completion of the incubation, 1% of 0.5 mg/mL MTT was added to each well and incubated for an additional 4 h. Culture medium was removed by centrifuge and 100 mL of DMSO/well was added. The formazan produced by reduction of MTT was determined by recording the absorbance of each well at 570 nm using Multiskan Ascent 354 microplate reader (Thermo Labsystems, Helsinki, Finland). Each experiment was repeated at least three times to get the mean values. The IC_{50} values were obtained from the dose–response curves using GraphPad PrismTM 5.0 software (GraphPad Software, Inc, La Jolla, California, USA).

Western blot analysis

A549 cells (1×10^5 /well) were pretreated with **6k**, **6l**, **7k**, and selumetinib (20 μM) for 4 h and stimulated with TGF- β (10 ng/L) for 10 min. Protein sample preparation and expression of phospho-ERK, total-ERK, and β -actin were examined by western blot analysis as previously described (Li et al. 2010). Briefly, whole-cell pellets were lysed in radio immuno precipitation assay lysis buffer [50 mM Tris (pH7.4), 150 mM NaCl, 1% Triton X-100, 1% sodium deoxycholate, 0.1% SDS, 1% NP-40, 1 mM sodium orthovanadate, 1 mM EDTA, 1 mM sodium fluoride, 100 mg/mL phenylmethylsulfonylfluoride, 100 mg/mL dithiothreitol (DTT)] at 4 °C for 30 min. The lysates were clarified by centrifugation at $10,000 \times g$ for 10 min at 4 °C. Protein concentration of the lysate samples was determined using Bio-Rad Protein Assay kit. Protein samples were separated by SDS-PAGE and transferred to polyvinylidene difluoride membranes (Millipore). The membranes were then blocked with 5% skimmed milk and incubated with primary antibodies: phospho-p44/42 MAPK (Thr202/Tyr204) antibody (1:1000; rabbit polyclonal; Cell Signaling, MA); p44/42 MAPK antibody (1:1000; rabbit polyclonal; Cell Signaling) overnight followed by washing. Where indicated, the blots were reprobated with antibodies against β -actin (Calbiochem) to ensure equal loading and transfer of proteins. The reaction was detected by IRDye[®] 800CW, conjugated goat (polyclonal) anti-mouse or rabbit antibody (LI-COR Biosciences, Lincoln, Nebraska USA) and visualized by Odyssey Scanner (LI-COR Biosciences, Lincoln, Nebraska USA).

Molecular docking

The molecular docking simulations were carried out using crystal coordinates from the X-ray crystal structure of MEK1 (PDB code: 1S9J), MEK2 (PDB code: 1S9I) obtained from the Protein Data Bank (Ohren et al. 2004). Compounds were built using the builder toolkit of MOE 2016 (Chemical Computing Group Inc, Canada) and the energy was minimized by force field of MMFF94. The protein crystal structures were prepared prior to docking in order to remove waters, add hydrogen atoms, remove atomic clashes and correct all structural items. Molecular docking analysis was performed by the Docking module of MOE package to confirm docking occurred between the flexible ligand parts of the compound and enzyme. The mode of construction for the docking was set to ligand. Other default parameters were adopted in the MOE-docking calculations. The binding energy involving H-bond interactions, hydrophobic interactions and van der Waal's interactions was described by London dG Scoring. Interactions between the compound and enzyme were explored by distance measurements.

Results and discussion

Chemistry

Compounds **6a–6l** and **7a–7l** were synthesized following the procedures described in Scheme 1. The isatin compound 2-oxoindoline-5-carboxylic acid (**3**) was constructed from the starting material 4-aminobenzoic acid (**1**) by reacting with trichloroacetaldehyde, hydroxylamine and concentrated sulfuric acid under the Sandmeyer isatin synthesis conditions (Bursavich et al. 2007). The ketone on 3-position of **3** was reduced to alkane (**4**) under Wolff-Kishner reduction conditions (Mologni et al. 2010). Compound **4** was then applied for amidation with aniline derivatives in the existence of TBTU as coupling agent to afford compounds **5a–5l** (de Candia et al. 2013). Final compounds **6a–6l** and **7a–7l** were obtained in good yields via coupling of

5a–5l with 1*H*-pyrrole-2-carbaldehyde or furan-2-carbaldehyde, respectively, under Knoevenagel reaction conditions (Kniess et al. 2009).

All titled compounds obtained were fully characterized by ¹H NMR and ¹³C NMR, and high resolution mass spectra (HRMS). The singlet protons in the ¹H NMR at around δ -10.20, -11.20 ppm in **7a–7l** and δ -10.20, -10.90 ppm in **6a–6l** and were characteristic to NH proton of isatin and amide, respectively. The singlet protons at around δ -13.2 ppm in **6a–6l** were attributed to pyrazoline. δ -7.89 ppm (**6a–6l**) and -8.19 ppm (**7a–7l**) were assigned to =CH protons. The ¹H NMR peaks in the range of δ 6.40–8.26 ppm (**6a–6l**) and 6.84–8.93 ppm (**7a–7l**) were due to different aromatic protons. In the ¹H NMR spectra of **6b–6d** and **7b–7d**, the singlet proton at δ 3.78 ppm were assigned to OCH₃ proton, whereas the singlets at δ 2.30 ppm in the ¹H NMR spectra of **6e–6g** and **7e–7g** were attributed to methyl group on the phenyl ring. All compounds have shown an excellent agreement between experimentally obtained and calculated data for HRMS analysis.

Structure–activity relationship

A549 human lung carcinoma cell line obtained from American Type Culture Collection (Rockville, MD, USA) was used for the cell proliferation assay with cisplatin and sunitinib as reference drugs. As shown in Table 1, compounds **6a**, **6c**, **6d**, **6j**, **6k**, **6l**, **7c**, **7g**, **7h**, **7i**, and **7k** displayed lower IC₅₀ values than cisplatin in cell proliferation assays. Compounds **6a**, **6k**, **6l**, and **7k** displayed equal activity in comparison to sunitinib, with the IC₅₀ value range of 3.0–4.1 μ M. Structurally, all compounds share similar chemical scaffold of 3-methylene-2-oxoindoline-5-carboxamide. The activity of compounds reported herein was dependent on the nature of the moiety present at the two different parts (Fig. 2). As for part I, the para-hydrogen bond acceptors on the phenyl group in part II can reverse the activity profiles for compounds **6** and **7**, such as p-OCH₃ (**6d/7d**), p-Cl (**6j/7j**), p-F (**6l/7l**).

Scheme 1 The synthesis of 3-methylene-2-oxoindoline-5-carboxamide derivatives **6a–6l** and **7a–7l**. Reagent and conditions: **a** Cl₃CCHO, NH₂OH.HCl, Na₂SO₄, 60–70 °C, 5 h; **b** H₂SO₄, 80 °C, 1 h; **c** NH₂NH₂, H₂O, 140 °C, 8 h; **d** DMF/DCM, TBTU, R-PhNH₂, 4-methylmorpholine, rt, 16 h; **e** furan-2-carbaldehyde or 1*H*-pyrrole-2-carbaldehyde, piperidine, 60 °C, 5 h

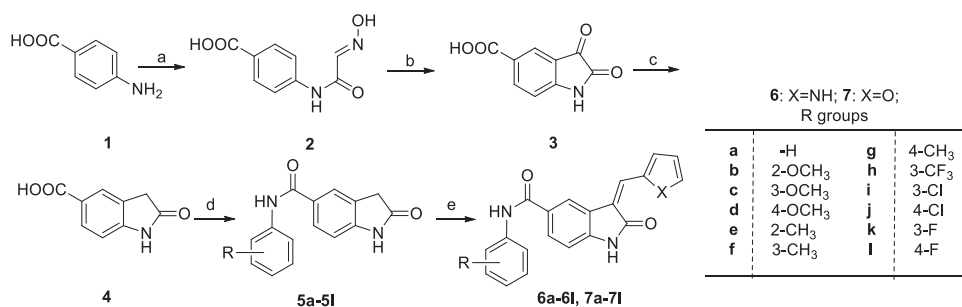


Table 1 The results of cell proliferation assay for compounds **6a–6l** and **7a–7l** and reference drugs

Compounds	IC ₅₀ (μM) ^a A549 cell line	Compounds	IC ₅₀ (μM) ^a A549 cell line
6a	3.9 ± 1.3	7a	10.4 ± 1.4
6b	27.1 ± 1.7	7b	13.0 ± 2.4
6c	7.9 ± 0.5	7c	6.2 ± 1.5
6d	8.5 ± 1.7	7d	13.9 ± 3.2
6e	15.3 ± 1.2	7e	14.0 ± 2.1
6f	30.0 ± 2.4	7f	12.9 ± 2.0
6g	19.8 ± 0.7	7g	6.2 ± 1.6
6h	13.3 ± 1.3	7h	7.2 ± 2.2
6i	14.7 ± 0.9	7i	6.5 ± 0.4
6j	9.9 ± 0.5	7j	57.5 ± 3.4
6k	3.3 ± 1.4	7k	4.1 ± 0.7
6l	3.0 ± 0.5	7l	25.5 ± 1.6
Cisplatin	10.2 ± 0.8	Sunitinib	2.3 ± 0.3

^a Values are means of three experiments, standard deviations are given

For pyrrole-containing compounds (**6a–6l**), most compounds displayed higher IC₅₀ values than **6a** (Table 1). Structurally, there is no any substituent on the phenyl group in part II for compound **6a** (Fig. 2, R=H, X=NH). For compounds **6b–6l**, the functionalities and positions of group attachment in this part displayed unfavorable effect. **6k** and **6l** are two exceptional compounds, which are also the two most potent compounds in this work. The possible reason lies in the special characteristics of fluorine atom, which has been extensively applied in drug design and discovery (Gillis et al. 2015).

For furan-containing compounds (**7a–7l**), compounds with hydrogen bond donor or electron-withdrawing groups attached on meta-position of phenyl group in Part II (Fig. 2) displayed higher potency than those with non-substitution (R=H, **7a**), such as **7c** (3-OCH₃), **7h** (3-CF₃), **7i** (3-Cl) and **7k** (3-F). Additionally, the para-position of phenyl group in part II need a methyl group to maintain the moderate activity, such as **7g** (4-CH₃).

Effect of active compounds on the phosphorylation of ERK1/2 in RAF/MEK/ERK pathway

To figure out whether the active compounds have the ability to regulate the components of RAF/MEK/ERK pathway, western blot analysis was applied to observe the p-ERK level for compounds **6k**, **6l**, **7k**, and selumetinib, a specific inhibitor of MEK1/2. A549 cells were treated with target compounds or selumetinib at 20 μM and then stimulated by TGF-β to obtain high concentration of RAF/MEK/ERK pathway components. As shown in Fig. 3, when compared

with TGF-β only group (negative control), all three compounds can inhibit TGF-β stimulated ERK 1/2 phosphorylation significantly. **6k** and **6l** displayed equivalent potency to selumetinib, which was also consistent with the results in anti-proliferation assay. The preliminary results indicated that 3-methylene-2-oxoindoline-5-carboxamide derivatives reported herein may inhibit the proliferation of A549 cell through regulation of phosphorylation of ERK1/2, the substrate of dual-function kinase MEK1/2 in RAF/MEK/ERK signaling cascade.

Molecular modeling studies

Since MEK1/2 is the kinase that regulates the phosphorylation of ERK1/2, it would be of necessity to get further insight into the binding mode of **6l** with MEK1 and MEK2. Compound **6l** was built and docked into the Asp-Phe-Gly (DFG) domain of MEK1 and MEK2 (Ohren et al. 2004). As shown in Fig. 4, compound **6l** fits well into the DFG-domain of both MEK1 and MEK2 with the binding energy of -23.6 and -21.6 kJ/mol, which can anchor **6l** to the allosteric site of the enzyme. The amine group of indolin-2-one interacts with the Asn82 residue of MEK2 through H-bond interaction with distance of 2.12 Å. The aromatic parts for indolin-2-one and aniline bind to MEK2 through π-hydrogen interactions with Lys101, Asp212, and Phe213, which is the DFG domain conserved in different sources of MEK2. Furthermore, the fluorine atom on the phenyl group of aniline form a weak bond with Val131 with distance of 3.60 Å, which would be of benefit to increase the affinity of **6l** to enzymes. Similarly, the carbonyl group of indolin-2-one and the NH of aniline interacts with Ile216 and Phe209 of MEK1 through H-bond interactions (2.41 and 2.40 Å), respectively. And the phenyl moiety of indolin-2-one group interact with Gly210 through π-hydrogen interaction. Likewise, the fluorine atom also interacts with Gly128 through weak bonding with distance of 3.13 Å. The molecular modeling studies also suggested that 3-methylene-5-carboxyl-indolin-2-one is a potential scaffold for the discovery of regulators of RAF/MEK/ERK pathway.

Conclusions

In summary, a series of 3-methylene-2-oxoindoline-5-carboxamide derivatives were synthesized by keeping the carboxyl group on the 5-position of indolin-2-one. In vitro biological assay indicated that both part I and part II are important structural determinants for the inhibitory activity against A549 cell proliferation, which also suggested a relationship between the anti-proliferative activity and blockade of the phosphorylation of ERK1/2. These results encourage that 3-methylene-2-oxoindoline-5-carboxamide

Fig. 3 The influence of compound **6k**, **6l**, and **7k** (20 μ M, respectively) on the phosphorylation of ERK1/2 with selumetinib (20 μ M) as positive control. A549 cell line was treated with compounds for 4 h and then stimulated with TGF- β (10 ng/L) for 10 min. p-ERK1/2, phospho-ERK1/2; t-ERK, total-ERK1/2

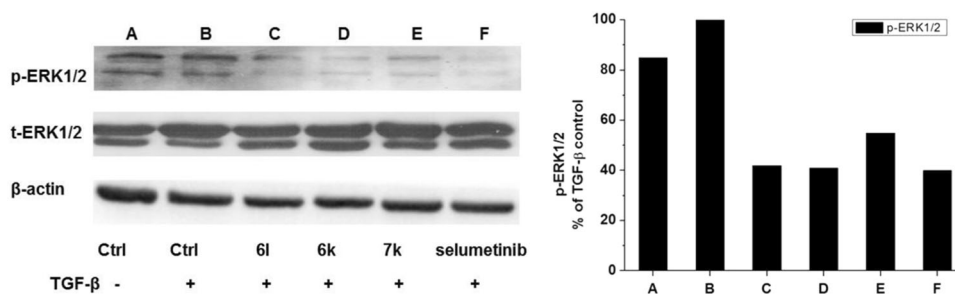
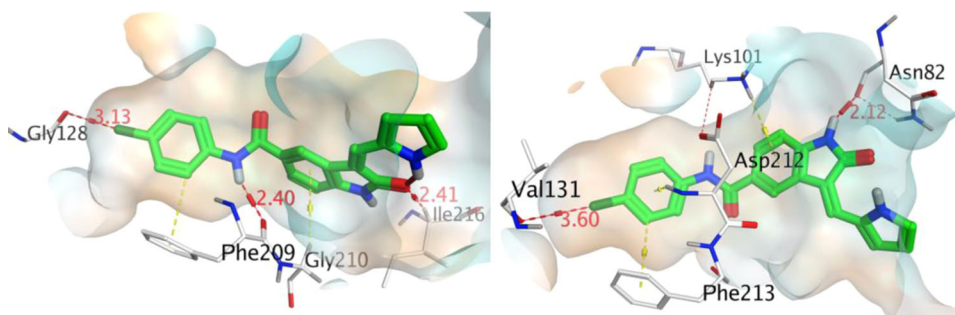


Fig. 4 The binding mode of compound **6l** to the DFG-domain of MEK1 (left) and MEK2 (right). The distance labels are in red, compound **6l** is in green, the residues of protein are in white. The molecular surfaces of both proteins are built with the color of lipophilicity (hydrophilic surface in cyan and lipophilic surface in orange) (color figure online)



is a promising scaffold for further structure modification and optimization, especially for the discovery of regulators of RAF/MEK/ERK pathway through inhibition of dual-function kinase and provide a new strategy for the development of anti-lung cancer agents.

Acknowledgements We would like to thank Dr. Dejian Jiang and his groups (Drug safety and evaluation research center, Hunan, China) for biological assays. This work was supported by National Nature Science Foundation of China (Grant No. 21102184), the Ph.D. Programs Foundation of Ministry of Education of China (No. 20110162120033), Nature Science Foundation of Hunan (Grant No. 2016JJ2162).

Compliance with ethical standards

Conflict of interest The authors declare that they have no competing interests.

References

- Abdel-Rahman O (2016) Targeting the MEK signaling pathway in non-small cell lung cancer (NSCLC) patients with RAS aberrations. *Ther Adv Respir Dis* 10:265–274
- Albaugh P, Fan Y, Mi Y, Sun F, Adrian F, Li N, Jia Y, Sarkisova Y, Kreusch A, Hood T, Lu M, Liu G, Huang S, Liu Z, Loren J, Tuntland T, Karanewsky DS, Seidel HM, Molteni V (2012) Discovery of GNF-5837, a selective TRK inhibitor with efficacy in rodent cancer tumor models. *ACS Med Chem Lett* 3:140–145
- Bursavich MG, Gilbert AM, Lombardi S, Georgiadis KE, Reifenberg E, Flannery CR, Morris EA (2007) 5'-Phenyl-3'H-spiro[indoline-3,2'-[1,3,4]thiadiazol]-2-one inhibitors of ADAMTS-5 (aggrecanase-2). *Bioorg Med Chem Lett* 17:5630–5633
- Davies H, Bignell GR, Cox C, Stephens P, Edkins S, Clegg S, Teague J, Woffendin H, Garnett MJ, Bottomley W, Davis N, Dicks E, Ewing R, Floyd Y, Gray K, Hall S, Hawes R, Hughes J, Kosmidou V, Menzies A, Mould C, Parker A, Stevens C, Watt S, Hooper S, Wilson R, Jayatilake H, Gusterson BA, Cooper C, Shipley J, Hargrave D, Pritchard-Jones K, Maitland N, Chenevix-Trench G, Riggins GJ, Bigner DD, Palmieri G, Cossu A, Flanagan A, Nicholson A, Ho JW, Leung SY, Yuen ST, Weber BL, Seigler HF, Darrow TL, Paterson H, Marais R, Marshall CJ, Wooster R, Stratton MR, Futreal PA (2002) Mutations of the BRAF gene in human cancer. *Nature* 417:949–954
- de Candia M, Fiorella F, Lopopolo G, Carotti A, Romano MR, Lograno MD, Martel S, Carrupt P-A, Belviso BD, Caliandro R, Altomare C (2013) Synthesis and biological evaluation of direct thrombin inhibitors bearing 4-(Piperidin-1-yl)pyridine at the P1 position with potent anticoagulant activity. *J Med Chem* 56:8696–8711
- Douillard JY, Rong A, Sidhu R (2013) RAS mutations in colorectal cancer. *N Engl J Med* 369:2159–2160
- Downward J (2003) Targeting RAS signaling pathways in cancer therapy. *Nat Rev Cancer* 3:11–22
- Espinosa AV, Porchia L, Ringel MD (2007) Targeting BRAF in thyroid cancer. *Br J Cancer* 96:16–20
- Gan HK, Seruga B, Knox JJ (2009) Sunitinib in solid tumors. *Expert Opin Investig Drugs* 18:821–834
- Gillis EP, Eastman KJ, Hill MD, Donnelly DJ, Meanwell NA (2015) Applications of fluorine in medicinal chemistry. *J Med Chem* 58:8315–8359
- Kammasud N, Boonyarat C, Sanphanya K, Utsintong M, Tsunoda S, Sakurai H, Saiki I, Andre I, Grierson DS, Vajragupta O (2009) 5-Substituted pyrido[2,3-d]pyrimidine, an inhibitor against three receptor tyrosine kinases. *Bioorg Med Chem Lett* 19:745–750
- Kammasud N, Boonyarat C, Tsunoda S, Sakurai H, Saiki I, Grierson DS, Vajragupta O (2007) Novel inhibitor for fibroblast growth factor receptor tyrosine kinase. *Bioorg Med Chem Lett* 17:4812–4818
- Kniess T, Bergmann R, Kuchar M, Steinbach J, Wuest F (2009) Synthesis and radiopharmacological investigation of 3-[4'-[(18)F]fluorobenzylidene]indolin-2-one as possible tyrosine kinase inhibitor. *Bioorg Med Chem* 17:7732–7742
- Li Q, Al-Ayoubi A, Guo T, Zheng H, Sarkar A, Nguyen T, Eblen ST, Grant S, Kellogg GE, Zhang S (2009) Structure–activity

- relationship (SAR) studies of 3-(2-amino-ethyl)-5-(4-ethoxybenzylidene)-thiazolidine-2,4-dione: development of potential substrate-specific ERK1/2 inhibitors. *Bioorg Med Chem Lett* 19:6042–6046
- Li Q, Wu J, Zheng H, Liu K, Guo TL, Liu Y, Eblen ST, Grant S, Zhang S (2010) Discovery of 3-(2-aminoethyl)-5-(3-phenyl-propylidene)-thiazolidine-2,4-dione as a dual inhibitor of the Raf/MEK/ERK and the PI3K/Akt signaling pathways. *Bioorg Med Chem Lett* 20:4526–4530
- Martinelli E, Morgillo F, Troiani T, Ciardiello F (2017) Cancer resistance to therapies against the EGFR-RAS-RAF pathway: the role of MEK. *Cancer Treat Rev* 53:61–69
- Mologni L, Rostagno R, Bruscolo S, Knowles PP, Kjaer S, Murray-Rust J, Rosso E, Zambon A, Scapozza L, McDonald NQ, Lucchini V, Gambacorti-Passerini C (2010) Synthesis, structure–activity relationship and crystallographic studies of 3-substituted indolin-2-one RET inhibitors. *Bioorg Med Chem* 18:1482–1496
- Ogawa H, Tamada S, Fujioka T, Teramoto S, Kondo K, Yamashita S, Yabuuchi Y, Tominaga M, Nakagawa K (1988) Studies on positive inotropic agents. V.: synthesis of 1-heteroaryl piperazine derivatives. *Chem Pharm Bull (Tokyo)* 36:2253–2258
- Ohren JF, Chen H, Pavlovsky A, Whitehead C, Zhang E, Kuffa P, Yan C, McConnell P, Spessard C, Banotai C, Mueller WT, Delaney A, Omer C, Sebolt-Leopold J, Dudley DT, Leung IK, Flamme C, Warmus J, Kaufman M, Barrett S, Teclé H, Hasemann CA (2004) Structures of human MAP kinase kinase 1 (MEK1) and MEK2 describe novel noncompetitive kinase inhibition. *Nat Struct Mol Biol* 11:1192–1197
- Pao W, Wang TY, Riely GJ, Miller VA, Pan Q, Ladanyi M, Zakowski MF, Heelan RT, Kris MG, Varmus HE (2005) KRAS mutations and primary resistance of lung adenocarcinomas to gefitinib or erlotinib. *PLoS Med* 2:e17
- Roberts PJ, Der CJ (2007) Targeting the Raf-MEK-ERK mitogen-activated protein kinase cascade for the treatment of cancer. *Oncogene* 26:3291–3310
- Schubbert S, Shannon K, Bollag G (2007) Hyperactive Ras in developmental disorders and cancer. *Nat Rev Cancer* 7:295–308
- Sun L, Tran N, Liang C, Tang F, Rice A, Schreck R, Waltz K, Shawver LK, McMahon G, Tang C (1999) Design, synthesis, and evaluations of substituted 3-[(3- or 4-carboxyethylpyrrol-2-yl)methylidene]indolin-2-ones as inhibitors of VEGF, FGF, and PDGF receptor tyrosine kinases. *J Med Chem* 42:5120–5130
- Sun L, Tran N, Tang F, App H, Hirth P, McMahon G, Tang C (1998) Synthesis and biological evaluations of 3-substituted indolin-2-ones: a novel class of tyrosine kinase inhibitors that exhibit selectivity toward particular receptor tyrosine kinases. *J Med Chem* 41:2588–2603
- Xu Q, Jiang X, Zhu W, Chen C, Hu G, Li Q (2016) Synthesis, preliminary biological evaluation and 3D-QSAR study of novel 1,5-disubstituted-2(1H)-pyridone derivatives as potential anti-lung cancer agents. *Arab J Chem* 9:721–735